Report No. IAEA – R – 4531–F

TITLE

$^{230}Th/^{234}U$ dating of the quaternary spring travertines in the Arava Rift Valley of Israel and paleoclimatic implications

FINAL REPORT FOR THE PERIOD

15 December 1986 – 15 December 1987

AUTHOR(S)

Joel Kronfeld

INSTITUTE

Tel Aviv University, Tel Aviv, Israel

INTERNATIONAL ATOMIC ENERGY AGENCY

DATE July 1988

$^{230}Th/^{234}U$ Dating of the Quaternary Spring Travertines of the Arava Valley, Israel

Final Report: Contract No. 4531/RB

International Atomic Energy Agency

Submitted by: Dr. Joel Kronfeld

Department of Geophysics and Planetary Sciences

Tel Aviv University, Ramat Aviv, Israel.

Abstract

Over 40 new $^{230}Th/^{234}U$ ages of travertines from the western Arava margins have been determined. Most fall within ^{18}O stages 5 and 7, confirming the findings of a previous study (Livnat & Kronfeld, 1985). Careful field, microscopic and SEM control of the dated samples, lend high credibility to the validity of the radiometric ages, and support the climatic conclusions drawn from them.

The travertines consist of two microfacial types: one is dominated by filamentous and coccoid cyanophytes, the other is characterized by macrophytes with abundant carbonate detritus. Textural evidence suggests that diagenesis was biochemically controlled and essentially occurred under phreatic conditions during immersion in the effluent water. Low-Mg calcite is the only carbonate phase, and it occurs both as micrite and sparite, whereas biogenic (gastropode) aragonite was dissolved during diagenesis. The limited degree of epigenetic recrystallization and dissolution, the absence of petrocalcic pedogenic horizons, the pendant-pore cementation, the preservation of cortical tissue of vascular plants, the minor aeolian quartz-clast contents, the stability of neoformed smectite and the absence of oolitic textures indicative of high-flow turbulence, all point to climatic amelioration (moderately arid) as compared to the present day extremely arid climate in the Arava. This conclusion is compatible with preliminary palynologic evidence and with paleosalinity estimates of the contemporaneous Lake Samra.

The temporal clustering of the inferred spring discharge maxima during the warm ^{18}O stages 5 and 7 bears smiliarity to the temporal distribution of sapropelic horizons in the eastern Mediterranean. These sapropels are attributed to anoxic events induced by extensive input of fresh water by the Nile during monsoonal maxima. Based on the temporal similarity we speculate that the intermittent spring-discharge pattern was modulated by migration of monsoonal cells during periods of insolation maxima to latitudes 30-31°N. The probability of monsoonal cell excursion from the present-day monsoonal belt during the early Holocene insolation maxima was predicted by climatic modelling and by the spatiotemporal inhomegeneity of climatic proxy data in the Near East. This intriguing climatic hypothesis needs further substantiation by combined palynologic and light-stable isotope study and by dating of travertines in Northern Israel.

1. Introduction

In a previous study, some spring- and lake-deposits of the Sayif Formation (Sneh, 1982), outcropping at two locations along the western margins of the northern Arava segment of the Dead Sea Rift Valley were U-series dated (Livnat & Kronfeld, 1985). It was demonstrated that for these localities spring discharge in the last 300,000 years was intermittent, as most of the $^{230}Th/^{234}U$ disequilibrium ages coincide with oceanic isotope stages 5 and 7. To the degree that these localities represent the arid south of Israel, the conclusion that during those periods "the arid south of Israel apparently was considerably wetter than at present" was tentatively confirmed by a palynologic study of some of the dated samples. The significantly higher than present-day ratio of Arboreal pollen vs. Non- Arboreal pollen was interpreted as indicative of more humid climate (Weinstein-Evron, 1987)such that discharge maxima could be reasonably attributed to climatic modulation rather than to poorly documented tectonic events (Horowitz, 1987; Livnat & Kronfeld, 1987).

In order to test the regional applicability of the age-clustering pattern and further examine its paleoclimatic significance, we sampled and dated by the $^{230}Th/^{234}U$ disequilibrium method additional spring and lake deposits from several localities, spanning most of the length of the western margins of the Arava (Fig. 1). In addition, the sampled travertines as well as representative samples of a previous study (Livnat & Kronfeld, 1985) were subjected to detailed mineralogic, chemical and petrographic study, in order to gain insight into possible

diagenetic or epigenetic changes to which the travertines may have been subjected and which could affect the U-series disequilibrium dating method.

2. General Setting

The Arava Segment of the Dead Sea Rift Valley is an extremely arid continental extension of the Dead Sea Transform (Fig. 1). It ranges in width between 32 km south of the Dead Sea (where elevation drops to 400 m below M.S.L.), and just a few kilometers at the internal water divide (225 m above M.S.L) about 77 km north of the Gulf of Elat. Northward of this divide, drainage heads towards the Dead Sea basin, whereas south of the divide most of the episodic runoff is lost by evaporation from several landlocked sabkhas. The eastern steep flank of the Arava is an expression of uplifted blocks outlined by normal faults which expose the Precambrian basement with an overlying arenaceous sequence of Paleozoic to Early Mesozoic age. The western margins of the Arava north of the regional water divide, are topographically milder and devoid of significant faulting. The transition towards the Negev Highlands occurs across a belt containing two types of structural elements: Some NNE plunging, asymmetric folds of Cretaceous to Tertiary age, and Tertiary structural domes. The oldest exposed rocks at the western Arava margins are some Jurassic carbonates which are overlain by Lower Cretaceous arenites, Upper Cretaceous to early Tertiary carbonates with subordinate luthitic, cherty and phosphoritic horizons, and Neogene to Recent clastic deposits (Fig. 2).

The annual precipitation in the Arava ranges between 50 mm in the north to 20 mm in the south (Maneh and Rozman, 1957). The current extreme aridity stems from the combined effect of the middle-latitudinal position within the high-pressure belt, and a lee-wind

position with respect to the westerlies. These moisture bearing winds undergo adiabatic heating upon an elevation drop of over a kilometer from the Negev Highlands to the Arava's rift bottom.

Present day spring discharge is commonly small, although substantial groundwater reservoirs are tapped by drilling. Much of the groundwater as well as runoff originate in the less arid, outlying highlands (where annual precipitation ranges between 100 and 300 mm). However, in the deeper aquifers, groundwater consists of essentially non-renewable reservoirs of Late Pleistocene age (Issar et al., 1972; Gat and Galai, 1982).

3. Site Geology

Appendix 1 summarizes the stratigraphic contacts and the topographic setting of the sample sites. The detailed stratigraphic and geographic relations of the samples are illustrated in Figures 3-7.

Outcrops range in size between several tens of square meters up to several square kilometers. Thickness, generally on the order of 0.5 to 6 meters, varies across small distances, commonly increasing from the interflooves towards the upper slopes of erosional channels. Outcrops usually slope several degrees and conform to the regional erosional surface . Most travertines overly much older rock units; however, in a few instances they are suprajacent to limestones or marls of lacustrine origin or to fluviatile deposits, inferred to be Pliocene or younger in age. In terms of the morphology of accumulations (cf. Hafetz and Folk, 1984), the Arava margin travertines can be classified

as mildly sloping mounds and fans.

The spatial disposition of adjacent travertine outcrops is determined by several parameters: the rate of carbonate deposition vs. the rate of erosion during the discharge periods; the temporally variable position of the groundwater table and the position of the spring deposits with respect to the local erosional base level. Hence for any given concurrent travertine deposit, elevation difference above the surrounding topography may range between ~1 and ~40 meters depending on its position with respect to the current local base-level. At several localities marginal to the Arava depocenter, some of the older travertines have been buried underneath prograding alluvial fans. Consequently, travertines of successive ages may form either a younging upwards, vertically continuous sequence, or alternatively, a younger deposit would occupy a topographically lower terrace with respect to an older one related to the same spring outlet. Hence, apparent ages based on field relations can be determined judiciously only for outcrops associated with a common drainage basin.

4. Sampling and Analytical Methods

Samples of travertines were collected from the Mahktesh Qatan southwards along the rift valley margins to Wadi Hiyyon-outlet at the sites indicated on the sample locator map (Figure 1). Sampling was geared towards establishing sound field control: at each site at least two, and up to five samples were collected from a given vertical succession, and in most localities at least two contiguous outcrops were sampled such that their relative position with respect to erosional surfaces would provide information concerning apparent ages. Wherever feasible, densely compacted samples with only minor secondary filling of vug spaces were analyzed. Careful field and petrographic control were combined with empiric corrections for detrital ^{232}Th, to provide an internally consistent set of radiometric dates.

From the samples of travertine that were collected in the field, approximately 50 were stained with Alizarin Red and studied in thin section using the petrographic microscope. From these samples forty were dated by the $^{230}Th/^{234}U$ method. As a supplementary petrographic aid to determine sedimentary textures and the chemical composition of allochtonous grains, most dated samples were studied using the Scanning Electron Microscope with an ion microprobe attachment. Approximately 75 travertine samples were analyzed by X-ray diffraction using a Phillips x-ray Diffraction Unit with Cu-K_α radiation to study their carbonate mineralogy. Of these, 45 were chemically analyzed for metal (Ca, Mg, Sr, Fe, Mn, Na and K) and stable trace metal (Cu, Ni and Zn) contents, using Atomic Absorption

permanently wet surfaces next to the spring outlets, with the presence

Spectrometry on a Perkin-Elmer Model 504 spectrophotometer.

Samples selected for isotopic analysis were first washed in an ultrasonic bath with distilled water to remove as much soluble salts, clay, and secondary calcite infilling as possible. Approximately 15-20 grams of dried material was then dissolved in 2N HNO_3. To the filtrate, a $^{234}U/^{228}Th$ spike and Fe^{+3} carrier were added, while the acid insoluble residue remaining on the filter paper was ashed and weighed. After the filtrate was precipitated at pH 9, using an ammonia solution, the radiometals were separated and purified using a combination of ion-exchange and solvent extraction techniques. The elemental uranium and thorium were each separately electroplated on stainless steel discs and subsequently analyzed by alpha-particle spectrometry. To determine the degree to which the uranium was effectively leached, aliquots of the samples were analyzed by delayed neutron activation (DNA).

alternation between active calcium carbonate deposition during day

Chemistry and Mineralogy

The results of the chemical analyses by atomic absorption are presented in Table 1. The metal composition of the travertines are reported as % or ppm by weight of the dry sample. National Bureau of Standards carbonate standards were used to check upon the accuracy of the AAS elemental analyses. Analyses of the standards are within the estimated uncertainty of the NBS analyses. Replicate analyses yielded values within 2-5% of each other. Therefore, the precision of these analyses is taken as between 2-5% of the reported values. The insoluble residue of most of the travertines was consistently within the range of 4-10%. The acid insoluble residue is predominantly clays and quartz grains. Significant exceptions to this is sample #2 (gypscrete) which yielded 49% insoluble residue, and samples #68/86 and #70/86 (lacustrine marly-chalks) which yielded between 17-20% insolubles. X-ray diffraction analysis revealed that the overwhelmingly dominant carbonate mineral is calcite. Mg-calcite molecule does not make up more than ~0.5 to ~1.5% of the total carbonate. Aragonite is absent. This is in agreement with the chemical data reported in Table 1 that show high Ca/Mg ratios in the travertines. Indeed, low Mg calcite is the stable carbonate phase to be expected to precipitate from the Arava-margin groundwaters, where generally rMg/rCa<1 (E. Rosenthal, written communication, 1987). The low Mg/Ca ratio in the regional groundwaters, the present-day strontium contents of the travertines ($\leq$ 0.2%) and the preservation of delicate

of intermittent discharge, confined primarily to the warm ^{18}O stages?

organogenic textures on a micro-scale, and the selective dissolution of gastropode shells of originally aragonitic composition, are all strong supports that the low Mg-calcite is not a replacement product of an aragonite precursor.

Secondary sulfates (primarily gypsum, some minor celestite) and halides (halite, sylvite?) were accounted only as late-paragenetic phases filling-in some primary and secondary pores. Their stability is to be expected under the current aridity of the region, and is further confirmed by the significant positive correlation between Na and K and the negative correlation between Na and Ca. Noticeably high concentrations of Na and K (amounting to 14% and 1%, respectively) were recorded in some marly lacustrine units near Moah and in the gypscretes of En-Erga (Fig. 5). The high values of Fe and/or Mn in the En-Zach and Makhtesh Qatan samples are compatible with the reported epigenetic mineralization at these localities. However, Cu, Ni and Zn are generally less abundant in the Makhtesh Qatan samples than at En Zach, which may be a result of both the dissimilarity in clay mineralogy and in the solution - chemistry of the epigenetic mineralization.

Radiometal Analyses

1 Thorium isotopes

Spring waters and the minerals precipitating from them are very low in thorium. In ideal cases for dating, no thorium isotopes are initially present. Uranium that is soluble and is precipitated along with the carbonate disintegrates and Th-230 is formed. The amount of thorium-230 present in a given sample, assuming a closed system, is a direct function of its half-life. However, an initial allogenic thorium component may be introduced along with the detrital material. If a significant amount of Th-232 is present it must be assumed that an initial quantity of Th-230 was also introduced, as both isotopes behave chemically the same way. Finite Th-230/Th-232 ratios exhibited in the samples are derived from leaching of the detrital component. If this is the principle source of the thorium contamination, the initial Th-230 introduced this way may be calculated for. An equation presented by Schwarcz (1980) has been used with the assumption that the initial Th-230/Th-232 ratio was approximately 1.5 (Table 3). This is the same correction used for the Negev Highland travertines (Schwarcz et al., 1979) and for the northern Arava travertines (Livnat and Kronfeld, 1985), and for the Lisan marls (Kaufman, 1971). The Th-230/Th-232 ratios in the preponderance of the samples were quite high. Age corrections would be, therefore, quite minor, irrespective of the exact initial ratio assumed. It is only when the ratios are in the range of less than approximately 10, that this correction takes on importance. There exists another source of detrital thorium that is more difficult to recognize and therefore correct for. This is the contamination by older carbonates such as limestones of the Judea Group

that originate from the surrounding hills. These carbonates are in secular equilibrium but contain virtually no Th-232. The microscopic thin section analysis detects such types of thorium contamination. Contamination of this type, if it has occurred, cannot be corrected for numerically. It's effect would be to yield older apparent absolute ages than warranted. As a case in point, we suspect that Sample #74/86, a young travertine, to judge from its topographic setting (Table 3), should in actuality have a true age that is somewhat younger still than is reported. It contains clasts of carbonates included within the travertine matrix. In the travertines used in this study microscopic analysis was reported on all dated samples and usually preceded chemical preparation.

2 Uranium

Uranium is much more mobile element in the supergene environment than is thorium. Ages can be affected by the subsequent mobilization or precipitation after the deposit was laid down. Additions (lowering of the apparent age) can take place if uranium is introduced a significant time after the induration of the deposit by coprecipitating with iron- or manganese - hydroxides as surface staining or as pore fillings. The ages can be altered to a degree dependent upon the quantity of uranium added as well as when it was added. Likewise, leaching of uranium can occur (as thorium is much less mobile, concomitant mobilization of Th-230 to the same degree as uranium would not be likely). Leaching would serve to raise the Th-230/U-234 ratio of the sample and therefore its apparent absolute age. If the uranium content was uniform during the time of incorporation for all

travertines or for the same time interval, subsequent additions or losses would be detectable. However, the uranium contents of the travertines studied here are very highly variable both in regard to their age as well as their geographical distribution. This variability is probably a reflection of initial conditions rather than post depositional effects for the majority of the samples-though. If post depositional effects have occurred, they may have affected the derived ages only in a small minority of the cases.

The high values of uranium (such as greater than 9 ppm in sample #57/86) are related to the presence of detrital phosphorite which is known to contain high uranium contents. The normal range, therefore, appears to extend approximately between 4.5 ppm to less than 0.4 ppm. The variability is probably related to an initial variability between sites in the uranium content of the source waters and/or to a difference in efficiency (Eh-pH conditions) of the individual spring pools in concentrating uranium.

The uranium content of the samples is variable. The reported range is from 9 to less than 0.4 ppm. However, the highest value may not be representative of the pure travertine. (For example, in Sample #57/86 which has a U-content in excess of 9 ppm). The uranium content of the travertines reported in Table 2 was determined after an acid leach. An acid insoluble fraction remains which is older than the carbonate. A total dissolution to release the radiometals that reside within their crystal lattice was not desirable. To determine the amount of uranium that was not leached from these detrital phases as

well as to reassure ourselves that the wide fluctuations in the U-content among the samples are real and not specious, seven samples were measured by delayed neutron activation (DNA). This method monitors the total uranium content. From Table 2 several observations are drawn: (1) The wide variation in the uranium content among the samples is real. In this sample population a variability factor of 5 among samples is demonstrated. (2) The difference between the two methods is not striking. The DNA analyses in six out of the seven samples are only slightly higher but not statistically significant. (3) Only one sample (#7/86) shows a significant difference between the two methods. Here almost a third of the uranium in this sample resides in a detrital phase that has not been leached. It can therefore be concluded that the acid leach employed is effective for releasing the uranium from the carbonate fraction. The leachable material can be considered to represent the travertine itself.

$^{230}Th/^{234}U$ Dating

The isotopic data of the study samples with the calculated ages are presented in Table 3. The statistical counting errors are reported at the 1 sigma level of confidence. All the data, excepting those which are either not datable, beyond the method, or incompatible with field relations (Sample #16/86) are presented in Fig. 8. These data are compared to published dates of the North Arava travertines (Livnat and Kronfeld, 1985), and to the Negev Highland travertine ages (Schwarcz et al., 1979). The spectrum of ages (analytically measured) includes samples whose formation age extends beyond the limits of the method. The age limits of the U-series method at present theoretically extend between about less than 5k yr to approximately 350k yr. However, because of inherent uncertainties about possible initial Th-230 additions coupled with relatively low uranium contents that resulted in lower counting statistics we take the upper limit for reporting ages as 300k yr for this study. The following observations are therefore noted:

1) Age distribution can be assigned to discrete clusters.
2) These clusters appear to fall within discrete intervals that are correlative to the oceanic oxygen isotope stages.
3) Even with a wider age distribution in evidence than noticed in the previous study, the major periods of travertine formation remain associated with stages 5 and 7.
4) Younger ages are also found. It is difficult to distinguish between the stages 2,3,4. The ages, though, fall within times of travertine formation in the Negev Highlands as well as the time of higher lake

levels of Lake Lisan (Kaufman, 1971).

5) The young ages, though, do not extend upwards into the Holocene. It appears that the Holocene was a period of non-significant travertine deposition. Most probably this reflects a period of reduced hydrological activity, apparently reflecting an aridity similar to the present day situation.

6) Older ages are reported than noted previously, that extend beyond 300,000 years. This lends support to the fact that the abundant representation of the older stage 7 is not due to a sampling bias. The samples representing older periods are more numerous than that for stage 9. This may be an artifact being close to the limit of the method. There is a large asymmetrical statistical error associated with the samples of older age. Consequently, overlaps of the error bars across age boundaries occur. This blurs the distinction between the groups at the older end of the scale.

7) The under-representation of most of the isotope stage 6 is striking. It is essentially a period of non-deposition of travertine.

8) From Fig. 8 it would appear that stage 8 is represented by three samples, making its representation as a period of travertine formation greater than previously suggested. However, inspection of the individual samples and comparison with the ages that stratigraphically bound them would indicate that there are doubts associated with the precision of these ages rather than indications that this stage was actually a period of significant deposition. In specific, sample #12/86 is a case in point. It is divided into two adjacent subsamples - top and bottom. Sample #12/86top sits immediately above sample #12/86bottom that yields an age coinciding with stage 7, and below

sample #13/86 that yields a lower stage 7 age. It should likewise be expected to yield an intermediate stage 7 age rather than its apparent stage 8 age. Petrographic analysis of the sample in thin section reveals an explanation for the discrepancy. It contains plentiful silt sized particles of older aeolian carbonate material. This wind transported contamination increased the apparent age of the sample.

Likewise, it is not possible to definitively assign the sample #26/86 to stage 8. It is stratigraphically younger than sample #24/86 that yields a stage 7 age. In both samples the error bars extend cross the adjacent age boundaries. This sample has to be younger than the lower sample. This may be a case of poor statistical precision associated with the lower counting rates that statistically enabled the age to fall within the lower range of the statistical error. No confidence can be attributed to a stage 8 age for this sample.

If the present samples are pooled with the age distributions previously determined from the Negev Highlands and the En-Yahav - En Rahel travertines, a rather consistent picture emerges of discrete times of travertine deposition. It can be concluded that: 1) The travertines are indeed stratigraphically associated with the Middle- to Late- Pleistocene. They extend to times older than 300,000 but do not continue into the Holocene; 2) most of the samples fall within an age range that is datable by the U-series method; 3) clusters are found that indicate that the times corresponding to oxygen isotope stages 5 and 7 were important for travertine formation. Stage 6 and stage 8 times were not; 4) the present work supports the contention of Livnat

and Kronfeld (1985) and of Weinstein-Evron (1987) that the times of travertine formation are climatically controlled. Travertine deposition represents periods of increased humidity compared to the present rather than to periods of drier conditions coupled with greater regional tectonic activity (uncovering "buried aquifers" as proposed by Horowitz 1987); 5) It appears that the travertines yield material that is valid for dating purposes by the U-series method. Most ages that are inconsistent stratigraphically can be explained by contaminations observed by petrographic analyses. Not all samples are valid dating material. Thin section analysis must precede the chemical procedure to cull out samples that may have iron staining, show weathering (leaching) effects, the presence of carbonate or phosphate clasts, or the extensive infilling of pores by secondary calcite.

. Discussion

1 Field and Petrographic Evidence for the Paleoclimatic and Environmental Setting of the Travertines

The field study and petrographic controls lend credibility to the isotopic age distribution exhibited by the Arava-margin travertines. The following observations are compatible with the intermittent nature of discharge of the studied spring outlets:

a) Most of the travertine ledges at any single locality represent discharge activity occuring over a short time span. Spring deposits indicative of an antecedent discharge at the site are displaced horizontally or vertically. This implyies a measurable drop of the

groundwater level, or/and incision of the drainage system followed by development of a new erosional surface in an intervening period of no or little discharge.

b) Some of the discrete travertine horizons (e.g. Nahal Hiyyon) are interlayered with pedogenic (gypsiferous) horizons.

Further information bearing on the paleoclimatic regime prevailing during and after the deposition of the studied travertines can be deduced from their petrography.

a) Often pore filling is incomplete

. The pore filling commonly consists of thin sparite rims or pendant (gravitationally induced) carbonate cement. It appears that after residing under submerged conditions (early diagenesis of the travertine's framework), the diagenetic processes proceeded under vadose conditions (cf. Longman, 1980). Corroborating evidence that the travertine was not fully submerged during this pore filling stage, is noted by the common occurrence of soluble salts (sulfates and halides) found within the infilling of some of the remaining pore-space after the deposition of the carbonate rims. This would tend to support the idea that diagenesis took place sequentially, from submerged to vadose conditions. It indicates that drying-out occurred in a very early stage of the pore-filling process.

b) The not uncommon preservation of organic, vascular-plant cortical remains inside the moldic pores that used them as templates, implying extended periods of low air humidity at the travertine sites. This retarded bacterially-induced and inorganic decomposition of the

Kutzbach, J.E., 1983. Monsoon rains of the Late Pleistocene and Early

organic matter.

c) Within many of the travertines a certain amount of clay- and silt-grade carbonate fraction is present. Only small scale, grain-boundary dissolution and recrystallization of the fine carbonate is observed. If they had been subjected to conditions of much significantly higher moisture than at present, such as a marginal Mediterranean climate (above ~300 mm/year precipitation), these carbonates would have tended to dissolve and recrystallize into a caliche crust or develop a petrocalcic soil horizon within a geologically short time (Dan, 1977). That this did not occur indicates that the moisture during the times of travertine deposition, while greater than at present, did not reach Mediterranean regime conditions.

d) The predominance of carbonate grains as the significant component of aeolian transport is also suggestive of aridity. There was no dissolutional elimination of these fine sized grains at the initial sites of their generation. The occasional occurrence of curled, or kinked clay flakes of presumably aeolian origin is a further evidence for aridity (Glennie, 1987). Secondary dissolution is generally very limited; where prevalent it is attributable to unique, and localized aquiferial conditions (e.g. the Makhtesh-Qatan).

e) To evaluate the importance of aeolian transport that prevailed during times of travertine formation, we have to look at the amount of wind transported quartz grains in the travertines, because is is difficult to distinguish between water-laid and wind-transported carbonate grains. Today, in the region, quartz-grains comprise in excess of 1/3 of the deposited aeolian material (Ganor, 1975). The

Roberts, N., 1982. Lake levels as an indicator of Near Eastern paleo-

permanently wet surfaces next to the spring outlets, with the presence of mucilagineous cyanophycean mats and vascular vegetation, should have provided efficient traps for aeolian deposits. Petrographic study reveals that the silt-sized, well sorted and angular quartz- grain population, believed to be of aeolian origin (Glennie, 1987), is of very low abundance. This may suggest that the Arava margins were in the deflation-dominated, "very-high wind erodibility zone" (Yaalon and Ganor, 1966), which is at present a reliable climatic index for < 200 mm annual precipitation. Would air humidity have been significantly higher, one would have encountered significant amounts of aeolian dust such as have accumulated, at least during the Late-Pleistocene onwards, along the northern margins of the Negev desert (the Loess belt; Yaalon and Dan, 1974; Issar and Bruins, 1983).

f) The stability of neoformed smectitic clays in the travertines is suggestive of a low degree of leaching (Singer, 1980).

g) The total absence of inorganic pisoids or algal oncoids, which normally grow under conditions of strong turbulence, is notable. Such textures are prevalent in travertines of northern Israel (Heiman, 1985, and unpublished data of the authors). The thick accumulation of these Pleistocene travertines precipitated from springs of large discharge (e.g. Bet Shean, Ga'aton, Banias-Dan).

h) Some of the radiaxial calcites nucleated around microphyte-peloidal nuclei, as well as some concentrically aligned, radial-calcite overgrowths around macrophyte-stem molds, bear evidence of rythmic deposition, described previously. The thickness of the microbanding in both documented cases has a similar range, namely between 5 and 10 μm. This microbanding may represent diurnal

Shmida, A., and Or, Y., 1983. The Sudanian Flora in Israel. Rotem, Botany Bulletin of the Society for the Protection of Nature in Israel.

alternation between active calcium carbonate deposition during day time, induced by some combination of biochemical (photosynthesis) and inorganic (evaporation induced by temperature increase) processes, and clastic-grain accumulation during night time when calcite saturation index and alkalinity were minimum. To the degree that the thickness of these microbands is representative, the average annual rate of calcite deposition is on the order of 1.8-3.6 mm/year. This is a rather slow rate as compared to values quoted as characteristic of some Pleistocene to Recent travertines in Italy and Idaho, namely 0.1 to 0.5 mm/day (Chafetz and Folk, 1983). Nevertheless, the rate calculated for the Arava travertines would have facilitated the accumulation of an average-thickness ledge of 2 meters within only 5.10^2 to $1.1 \cdot 10^3$ years.

Although none of the aforementioned observations can serve as a sound paleoclimatic indicator of its own, the combined evidence is supportive of a climatic regime in the Arava, that was only marginally wetter than at present, namely a moderately arid climate as contrasted with the present day extremely arid climate. A concomitant increase of humidity in the outlying highlands would have resulted in a significant expansion of the Mediterranean maquis (Weinstein-Evron, 1987) in areas that are at present dominated by desert or dry-steppe plant communities.

The combined evidence strongly supports, therefore, intermittent discharge pulses modulated by climatic variation with a moderate increase of humidity during the spring-discharge maxima episodes. What viable climatic model could be invoked to reasonably explain this type

List of Figures

of intermittent discharge, confined primarily to the warm ^{18}O stages?

2 Speculations considering the Paleoclimatic regime

A variety of studies of Wurmian and early Holocene climatic proxy-data (extinct lake levels, palynology, dune migration) have demonstrated that the late Quaternary-Early Holocene climatic record in the Near East was not spatiotemporally homogeneous (Roberts, 1982, 1983; Rossignol-Strick et al., 1982). These findings led to the realization that the effect of the northern ice-sheet dynamics on the uniform migration of climatic belts northwards (during interglacials) and southwards (during glacials) is an oversimplified concept, and that climatic proxy data of low latitudes are less directly dependent on ice sheets than was previously assumed. With the aid of climatic modelling based on linear climatic forcing by obliquity and non-linear eccentricity it was demonstrated that in the Late Pleistocene - early Holocene, periods of maximum insolation coincided with intensification and northward migration (up to >30°N) of low pressure cells above Asia and North Africa, which in turn induced a northward migration of Hedley cells (Kutzbach, 1983; Kutzbach and Street-Perott, 1985). For instance, Roberts (1982, 1984) demonstrated that the significant inter-regional lake-level fluctuations and chronological regularities in the Near East cannot be correlated directly with paleotemperature changes during the period between 6000 and 9000 yr BP. During this period lake levels south of latitude 28°N were high, whereas the northern zone of the Near East witnessed a period of low lake levels. This observation has led Roberts (1982) to conclude that "this was undoubtedly a product of a climatic regime different from that of the

Table 1: Major and trace element composition of the Arava travertines

Sample Code	Ca	Mg	Sr	Fe	Mn	Na	K	Cu	Ni	Zn

present day, in which the intertropical convergence zone lay around 10° north of its modern position. Tropical monsoonal rain affected the Saharan and Arabian desert...". Sand dune activity periods in the Sahara support the climatic modelling of Kutzbach (1983) (Sarnthein, 1978; Pakras and Mix, 1985). Changes in seasonal insolation were invoked (Spaulding & Graumlich, 1986) to explain the anomalously late persistence into the early Holocene of woodland in low latitude, low elevation deserts of the southwestern USA due to monsoonal circulation.

Rossignol-Strick (1983) demonstrated that eleven documented sapropelic events in the eastern Mediterranean during the last 464.10^3 years coincide with those periods when the northern summer monsoon index, computed from the orbital variation of insolation, reached maximum values. The sapropelic events were dated by comparison to the ^{18}O stratigraphy of core RC 9-181 in the eastern Mediterranean (Ryan 1972) using the chronostratigraphy of Morley and Hays (1981). Most of the summer monsoonal maxima coincide with the odd ^{18}O stages; however, two of them occurred during even ^{18}O stages; Rossignol-Strick (1983) attributed these sapropelic events to maxima of monsoonal precipitation at the Nile sources, with flooding leading to stable, density-caused stratification, a brackish epilimnion and development of stagnant bottom conditions in the eastern Mediterranean basin.

Although the analytical uncertainty of our U-series dates prevents a precise chronologic correlation between the Arava margin spring deposits and the eastern Mediterranean sapropelic events, we suggest

that the intermittent spring activity of the Arava margins reflects maximum northerly excursions of monsoonal cells to latitude 30°-31°N during the cited periods of maximum insolation events. We find it highly significant that those spring-activity records which deviate from the odd ^{18}O stages (namely, travertines deposited during late stage 6) coincide with the monsoonal maximum represented by Sapropel-6 as calculated by Rossignol-Strick (1983).

The Arava-margin spring activity is rather poorly represented during ^{18}O stage-3, although stage-3 was a period of discharge in the Negev Highlands (Schwarcz et al., 1979). We suspect that this reflects sampling bias, whereby some topographically low lying travertine outcrops of inferred "young" ages were avoided because they could not provide a satisfactory vertical succession of samples to assure field-control. This assumption is currently under examination. As to the climatic scenario during stage-3, while there were probably no monsoonal maxima events in the study area and its vicinity (there is no record of sapropelic events in the eastern Mediterranean during $\delta^{18}O$ stage-3; Rossignol-Strick, 1983), there is ample evidence for higher than present-day precipitation in the Sinai and the Negev at that period, probably due to southward migration of cyclonic cells (Gat and Magaritz, 1980; Gat, 1983; Issar and Bruins, 1983, Magaritz, 1986).

10. Summary and Conclusions

Sporadic outcrops of spring and lake deposits along the western margins of the Arava, occur in an area which at present is extremely arid (20-50 mm/y). Whereas some of the travertine sites are adjacent

to, and just at a slightly higher elevation than contemporary groundwater level, some others are dissociated from present-day spring outlets.

The Nahal Amazyahu lacustrine limestone lense represents a small, short-lived lake, with rythmic deposition of alternating clay-poor and clay-rich, low-Mg calcite laminae, and bears evidence for terminal dessiccation. Most travertines consist of two microfacial types with vertical and lateral intergradations: a microphyte-dominated facies (filamentous- and coccoid-cyanophytes and bacteria?), and a facies dominated by carbonate detritus. Detailed microscopic and SEM textural evidence is suggestive of biochemically-induced deposition of very low Mg-calcite, with deposition by inorganic processes (evaporation?) playing a subordinate role. Primary porosity is largely unoccluded by carbonates, but contains variable degrees of filling by sulfates and halides. Some minor vadose cementation and small amount of authigenic smectite are the most prevalent representatives of late-diagenetic processes. Epigenetic mineralization, involving the deposition of Fe and Mn (hydro) oxides, Al (hydro?) oxides, celestite and barite, is confined to two travertine sites, apparently associated with the upwelling of Nubian- aquifer waters during periods of low piezometric head.

A variety of petrographic observations points to deposition under intermittent, moderately-arid conditions, alternating with arid to extremely arid periods when spring-discharge ceased. These include: (1) the interlayering with pedogenic, gypsiferous horizons; (2) the

very limited carbonate recrystallization and karst-dissolution; (3) the small degree of carbonate pore filling associated with sulfates and halides; (4) the absence of petrocalcic pedogenic horizons; (5) the preservation of some cortical- organic relicts of vascular plants; (6) the minor aeolian quartz-clast contribution; (7) the stability of authigenic smectitic clay; (8) the absence of oncoid and pisoid textures indicative of flow-turbulence, and finally, (9) the short duration of deposition inferred from calculations of rate of deposition. This combined evidence is consistent with the preliminary palynological conclusions of moderately increased humidity (Weinstein-Evron, 1987), as well as with the paleosalinity estimates (Gardosh, 1987) of the contemporaneous Lake Samra (Kaufman, in Yechieli, 1987).

Dating by the $^{234}Th/^{230}U$ disequilibrium method indicates that some travertines outdate the applicability of the method (> 300 ka), with most travertine ages corresponding to ^{18}O stages 5 and 7. The good correspondence between apparent ages as deduced from the position of the travertines in vertical and lateral successions and the radiometric ages, lends credibility to the radiometric ages. Textural evidence suggests that the ages are believed to faithfully represent depositional time. Diagenesis appears to be virtually contemporaneous with deposition. Once formed, there was only a small degree of fluid-mobility in the travertines. Most of the U is retained in the soluble carbonate fraction, which was subsequently efficiently extracted during radiometric analysis. Radiometric ages which are incompatible with field-relations of the dated samples are generally denoted by their high allogenic carbonate contamination.

The clustering of ages during the odd (warm) ^{18}O stages bears similarity (within the analytical age uncertainty) to the temporal distribution of Middle- to Late-Pleistocene sapropelic horizons in the Eastern Mediterranean basin. These sapropels were attributed to anoxic events induced by high-flood events of the Nile due to intensive monsoonal rains, during periods of global-insolation maxima (Rossignol-Strick, 1983). The chronologic correspondence between the marine and terrestrial indices for abnormally high precipitation in the low latitudes of the northern hemisphere during ^{18}O stages 5 and 7 warrants the speculation that during insolation maxima of these stages, monsoonal cells originating in the Indian Ocean, have shifted northwards reaching the latitude of the Arava and Negev Highlands (30-31°N); the pulses of increased humidity resulted in corresponding pulses of the groundwater level, leading to an intermittent pattern of spring discharge. The viability of the hypothesis invoking long-range monsoon-cell shifts during odd-oxygen stages was demonstrated for the early Holocene by climatic modelling (Kutzbach, 1983), and is compatible also with the absence of spatiotemporal homogeneity of climatic-proxy data across the Near East during the Holocene (Roberts, 1982).

It is suggested that further testing of the monsoonal-migration hypothesis should be carried out by a systematic palynologic search of the Arava travertines for phyto-elements of Sudanian affinity (cf. Shmida and Or, 1983), and by radiometric dating and palynologic study of the travertine sites in northern Israel, to decipher their spring-

discharge history and epigenesis.

References

Bentor, Y.K., Kastner, M. and Mazor, E., 1966. The hydrothermal kaolinite of Makhtesh Ramon: In: The Clays of Israel, Guide book to the excursions, Y.K. Bentor (ed.); Israel Programs for Scientific Translations, 23-28.

Bignot, G., 1978. Illustration and paleoecological significance of Cretaceous and Eocene Girvanella limestones from Isria (Yugoslavia, Italy). In: Spec. Pub. Int. Ass. Sediment. 2, 134-139.

Buchbinder, B., 1981. Morphology, microfabric and origin of stromatolites of the Pleistocene precursor of the Dead Sea, Israel. In: Monty, C. (ed): Phanerozoic Stromatolites, Springer-Verlag, 181-196.

Carpelan, L.H. 1967. Daily alkalinity changes in brackish desert pools. Int. J. Oceanol. & Limnol. 1, 165-193.

Chafetz, H.S., and Folk, R.L., 1984. Travertines: Depositional morphology and the bacterially constructed constituents. Jour. Sed. Petrology, 54, 289-316.

Choquette, P.W., and Pray, L. 1970. Geologic nomenclature and classification of porosity in sedimentary carbonate. Am. Assoc. Petrol. Geol. Bulletin, 54, 207-250.

Dunham, R.J., 1969. Early vadose silt in Townsend mound (reef), New Mexico. In: Depositional Environments in Carbonate Rocks, Friedman, G.M. (ed.) Soc. Econ. Paleontologists and Mineralogists Spec. Pub. 14, 139-181.

Dunham, R.J., 1971. Meniscus cement. In: Carbonate Cements, Bricker, O.P. (ed.), Baltimore, John Hopkins University Press, 297-300.

Eidelman, A., 1979. The Geology of the Arava Rift margin in the En Yahav region. M.Sc. Thesis, Hebrew University of Jerusalem (in Hebrew, English abstract).

Eugster, H.P., and Hardie, L.A., 1978. Saline Lakes. In: Lakes, Chemistry, Geology, Physics, A. Lerman (ed.) Springer-Verlag, New York, 237-293.

Folk, R.L., and Assereto, R., 1976. Comparative fabrics of length-slow and length-fast calcite and calcitized aragonite in a Holocene speleothem, Carlsbad Caverns, New Mexico. Jour. Sed. Petrology, 46, 486-496.

Folk, R.L., and Chafetz, H.S., 1983. Pisoliths (Pisoids) in Quaternary travertine of Tivoli, Italy. In: Coated Grains, T.M. Peryt (ed.), Springer-Verlag Berlin Heidelberg, 474-487.

Ganor, E., 1975. Atmospheric dust in Israel - Sedimentological and Meteorological Analysis of Dust Deposition. Ph.D. Thesis, Hebrew University of Jerusalem (in Hebrew, English abstract).

Gardosh, M., 1987. Water composition of Late Quaternary lakes in the Dead Sea Rift. Isr. Jour. Earth Sci. 36, 83-90.

Gat, J.R., 1983. Precipitation and surface waters. In: Paleoclimates and Paleowaters: A Collection of Environmental Isotope Studies. International Atomic Energy Agency, Vienna, 3-12.

Gat, J.R., and Galai, A. 1982. Groundwaters of the Arava Valley: an isotopic study of their origin and interrelationships. Isr. Jour. Earth Sci., 31, 25-38.

Gat, J.R., and Magaritz, M., 1980. Climatic variations in the eastern Mediterranean Sea area; Naturwissenschaften 67, 80-87.

Gill, D., 1965. Petrographic study of some carbonate rocks from Jurassic outcrops in Makhtesh Qatan, southern Israel. Isr. Jour. Earth Sci., 14, 122-138.

Glennie, K.W. 1987. Desert sedimentary environments, present and past - a summary. Sedim. Geol. 50, 135-165.

Goldberg, M., 1967. Supratidal dolomization and dedolomitization in Jurassic rocks of Hamakhtesh Haqatan, Israel. Jour. Sed. Petrology, 37, 760-773.

Golubic, S., 1976a. Organisms that build stromatolites. In: Stromatolites, Developments in Sedimentology 20, M.R. Walter (ed.), Elsevier, New York, 113-126.

Golubic, S., 1976b. Taxonomy of extant stromatolite-building cyanophytes. In: Stromatolites, Developments in Sedimentology 20, M.R. Walter (ed.), Elsevier, New York, 113-126.

Grover, G. Jr. and Read, J.F., 1978. Fenestral and associated vadose diagnetic fabrics of tidal flat carbonates, Middle Ordovician New Market Limestone, southwestern Virginia. Jour. Sed. Petorlogy, 48, 453- 473.

Hanley, J.H., and Steidtmann, J.R., 1973. Petrology of limestone lenses in the Casper Fm., southernmost Laramie basin, Wyoming and Colorado. Jour. Sed. Petrology, 43, 428-434.

Heiman, A. 1985. The Geology of the Northern Hula Valley with emphasis on ancient spring deposits (travertines). M.Sc. Thesis, Hebrew University, Jerusalem (in Hebrew).

Hemley, J.J., Hostetler, P.B., and Gude, A.J., 1969. Some stability relations of alunite. Econ. Geol. 64, 599-612.

Horowitz, A., 1987. Travertines of arid regions, oxygen isotope stages, and Late Quaternary climates of Israel. Quat. Research, 27, 103-105.

Ilani, S., in prep. Epigenetic mineralization along tectonic lineaments in Israel. Ph.D. Thesis, to be submitted to the Hebrew University of Jerusalem (Hebrew, English abstract).

Issar, A., 1985. Fossil water under the Sinai-Negev Peninsula. Scientific American, 104-110.

Issar, A., Bein, A., and Michaeli, A. 1972. On the ancient water of the Upper Nubian Sandstone aquifer in central Sinai and southern Israel. Jour. Hydrology, 17, 353-374.

Issar, A.S. and Bruins, H.J., 1983. Special climatological conditions in the deserts of Sinai and the Negev during the latest Pleistocene. Paleogeog., Paleoclim., Paleoecol. 43, 63-72.

Issar, A., and Gross, S., 1969. A note on the possible origin of the so-called karstic caves at Ma'ale Hameshar in the central Negev. Isr. Jour. Earth Sci., 18, 29-32.

Issar, A., Rosenthal, E., Eckstein, Y. and Bogoch, R., 1971. Formation waters, hot springs and mineralization phenomena along the eastern shore of the Gulf of Suez. Bull. Intern. Assoc. Sci. Hydrol., XVI, 25-44.

Kaufman, A., 1971. U-series dating of Dead Sea Basin carbonates. Geochim. et Cosmochim. Acta, 35, 1269-1281.

Kelts, K. and Hsu, K.J., 1978. Freshwater carbonate sedimentation. In: Lakes, Chemistry, Geology, Physics. A. Lerman (ed.), Springer-Verlag, New York, 295-323.

Kendall, A.C., and Broughton, P.L. 1978. Origin of fabrics in speleothems composed of columnar calcite crystals. Jour. Sed. Petrology, 48, 519-538.

Klappa, C.F., 1979. Calcified filaments in Quaternary calcretes: organo-mineral interactions in the subaerial vadose environment. Jour. Sed. Petrology, 49, 955-968.

Kobluk, D.R., and Risk, M.J., 1977. Calcification of exposed filaments of endolithic algae, micrite envelope formation and sediment production. Jour. Sed. Petrology, 47, 517-528.

Krumbein, W.E., 1979. Photolithotropic and chemoorganotrophic activity of bacteria and algae as related to beack rock formation and degradation (Gulf of Aqaba, Sinai). Geomicrobiology Journal, 1, 139-203.

Kutzbach, J.E., 1983. Monsoon rains of the Late Pleistocene and Early Holocene; patterns, intensity and possible causes of changes. In: Variations in the Global Water Budget. A. Street-Perrott et al. (ed.) D. Reidel Publishing Co., 371-389.

Kutzbach, J.E., and Street-Perrott, F.A. 1985. Milankovitch forcing of fluctuations in the level of tropical lakes from 18 to 0 Kyr BP, Nature, 317, 130-134.

Livnat, A., and Kronfeld, J. 1985. Paleoclimatic implications of U-Series dates for lake sediments and travertines in the Arava Rift Valley, Israel. Quat. Research, 24, 164-172.

Livnat, A., and Kronfeld, J., 1987. Reply to comment on "Travertines of the Arid Regions, Oxygen Isotope Stages and Late Quaternary Climates of Israel" by A. Horowitz. Quat. Research, 27, 106-107.

Logan, B.W., 1974. Inventory of diagenesis in Holocene-Recent carbonate sediments, Shark Bay, Western Australia: In: Evolution and Diagenesis of Quaternary Carbonate Sequences, Shark Bay, Western Australia. Logan, B.W. (ed.), Am. Assoc. Petroleum Geologists Memoir 22, 195-249.

Longman, M.W., 1980. Carbonate diagenetic textures from near surface diagenetic environment. Amer. Assoc. Petrol. Geologists Bulletin 64, 461-487.

Magaritz, M., 1986. Environmental changes recorded in the Upper Pleistocene along the desert boundary, southern Israel. Paleogeog., Paleoclim., Paleoecol. 53, 213-229.

Maneh, E. and N. Roznan, 1987. "Map of the Annual Rainfall in Israel". Sheet 2IV,, Atlas of Israel, Department of Surveys, Jerusalem.

Morley, J.J. and Hays, J.D. 1981. Towards a high resolution, global, deep sea chronology of the last 750,000 years. Earth and Plan. Sci. Letters 53, 279-295.

Müller, G. 1971. Gravitational cement: An indicaor for the vadose zone of the subaerial diagenetic environment. In: Carbonate Cement, Bricker, O.P. (ed.), Baltimore, John Hopkins University Press, 301-302.

Müller, G., Irion, G. and Förstner, U., 1972. Formation and diagenesis of inorganic Ca-Mg carbonates in the lacustrine environment. Naturwissenschaften 59, 158-164.

Nickel, E., 1983. Environmental significance of freshwater oncoids, Eocene Guarga Formation, southern Pyrenees, Spain: :In Coated Grains, T. Peryt (ed.), Springer-Verlag, 308-329.

Riding, R., 1977. Calcified Plectonema (blue-green algae), a recent example of Cirvanella from Aldabra Atoll. Paleontology, 20, 33-46.

Roberts, N., 1982. Lake levels as an indicator of Near Eastern paleoclimates, a preliminary appraisal. In: Paleoclimates, Paleoenvironments and Human Communities in the Eastern Mediterranean Region in Later Prehistory, J.L. Printliff and W. Van Zeist (eds.), BAR International Series 133, 235-267.

Roberts, N., 1983. Age, paleoenvironments and climatic significance of Late Pleistocene Konya Lake, Turkey. Quat. Research, 19, 154-171

Roberts, N., 1984. Reply to comments by Ann P. El-Moslimany. Quat. Research, 21, 117-120.

Rosenthal, Y., and Katz, A., 1987. Utilization of ion ratios in Gastropode shells as paleogeochemical indicators. Proceed. Israel Geol. Soc. Ann. Meet., Mizpe Ramon, 114 (abst.)

Rossignol-Strick, M., Nesteroff, W., Olive P., and Vergnaud-Grazzini C., 1982. After the deluge: Mediterranean stagnation and sapropel formation. Nature, 295, 105-109.

Ryan, W.B.F., 1972. Stratigraphy of Late Quaternary sediments in the eastern Mediterranean. In: The Mediterranean Sea: A Natural Sedimentation Laboratory, Stanley, O.J. (ed.), Stroodsburg, Pa., Dowden, Hutchinson & Ross, 149-169.

Sarnthein, M., 1978. Sand deserts during glacial maximum and climatic optimum. Nature 272, 43-46.

Schneider, J., 1977. Carbonate Construction and Decomposition by Epilithic and Endolithic Micro-organisms in Salt and Freshwater. In: Fossil Algae, E. Flugel (ed.), Berlin, Springer-Verlag, 248-260.

Schoeller, H., 1977. Geochemistry of groundwaters. In: Groundwater Studies - An International Guide for Research and Practice. Unesco, Paris, ch. 15, 1-18.

Scholle, P.A. 1978. A Color Illustrated Guide to Carbonate Rock Constituents, Textures, Cements and Porosities. Am. Ass. Petroleum. Geologists. Memoir 27.

Schwarcz, H.P. 1980. Absolute age determination of archeological sites by uranium series dating of travertines. Archeometry 22 (1), 3-24.

Schwarcz, H.P., Blackwell, B., Goldberg, P., and Marks, A.E. 1979. Uranium series dating of travertine from archeological sites, Nahal Zin, Israel. Nature 277, 558-560.

Segev, A., 1984. Gibbsite mineralization and its genetic implication for the Um Bogma manganese deposit, Southwestern Sinai. Mineral Deposita 19, 54-62.

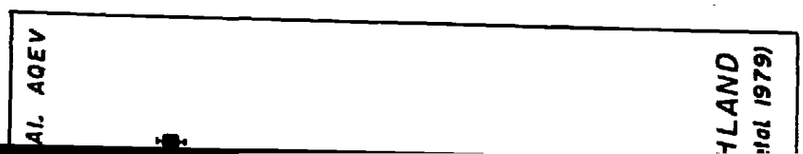

Shmida, A., and Or, Y., 1983. The Sudanian Flora in Israel. Rotem, Botany Bulletin of the Society for the Protection of Nature in Israel, No. 8, 150 pp (in Hebrew, English abstract).

Singer, A., 1980. The paleoclimatic interpretation of clay minerals in soils and weathering profiles. Earth-Science Reviews, 15, 303-326.

Sneh, A., 1982. Quaternary of the Northwestern Arava, Israel. Isr. Jour. Earth Sci. 31, 9-16.

Spoulding, W.G., and Graumlich, L.J., 1986. The last pluvial climate episode in the deserts of southwestern North America. Nature, 320, 441-444.

Weinstein-Evron, M. 1987. Palynology of Pleistocene travertines from the Arava Valley, Israel. Quat. Research, 27, 82-88.

Welton, J.E., 1985. SEM Petrology Atlas. Am. Assoc. Petroleum Geologists, Tulsa, Oklahoma, 237 pp.

Wilson, M.D. and Pittman, E.D., 1977. Authigenic clays in sandstones: recognition and influence on reservoir properties and paleoenvironmental analysis. Jour. Sed. Petrology, 47, 3-31.

Yaalon, D.H. and Dan, J., 1974, Accumulation and distribution of loess-derived deposits in the semi-desert and desert fringe areas of Israel. Z. Geomorph. Supp. Bd. 20, 91-105.

Yaalon, D.H. and Ganor, E. 1966. The climatic factor of wind erodibility and dust blowing in Israel. Isr. Jour. Earth-Sci. 15, 27-32.

Yechieli, Y., 1987. The geology of the northern Arava Rift and the Mahmal anticline, Hatzeva region. M.Sc. Thesis, The Hebrew University of Jerusalem (in Hebrew, English abstract).

Fig

Fig

Fig

Fig

Fig

Fig

Fig

Fig

List of Figures

Table 1: Major and trace element composition of the Arava travertines

Sample Code Number	Ca %	Mg %	Sr ppm	Fe ppm	Mn ppm	Na ppm	K ppm	Cu ppm	Ni ppm	Zn ppm
1	38.8	0.68	1690	1920	22	400	248	11	16	16
2	12.7	1.21	1140	5060	107	140000	2610	11	17	18
5	40.3	0.52	1360	3220	54	1880	196	4	27	23
6	35.5	0.42	1160	998	35	786	271	5	19	41
9	35.5	0.79	2260	1090	28	1020	1510	8	17	18
10	36.6	0.84	1920	847	51	2190	660	5	3	18
11	36.9	0.66	2480	1510	36	752	289	5	16	15
13	37.7	0.59	1150	2950	64	1340	1080	13	18	23
14	35.6	0.36	1180	2020	30	360	280	6	n.d.	17
18	35.8	0.63	1950	2080	40	1120	448	13	6	108
20	35.9	0.30	432	860	16	800	220	9	16	100
21	36.6	0.45	554	3360	117	356	764	15	31	82
28	38.9	0.34	1670	1550	39	631	339	10	19	125
7/86	35.7	0.71	1200	7130	65	594	293	47	82	711
8/86	34.6	0.61	1180	6532	53	880	640	41	48	482
12/86-Bot.	36.1	0.49	944	1960	33	600	440	50	6	107
12/86-Top	35.4	0.51	1130	1740	33	792	341	25	8	87
13/86	35.0	0.51	1240	1320	45	560	356	44	9	78
16/86	38.2	0.50	1080	284	28	1320	100	51	10	90
17/86	36.0	0.44	684	1090	52	640	192	34	9	128
20/86	35.9	0.35	612	1430	52	5850	378	14	4	68
22/86	35.3	0.44	1350	394	16	636	123	12	12	86
24/86	35.2	0.31	726	690	29	11400	159	17	8	71
25/86	35.3	0.44	962	1670	33	397	441	15	12	118
26/86	38.4	0.52	1250	868	22	2560	192	10	7	70
45/86	35.5	0.62	1540	4250	162	1073	437	14	11	19
46/86	37.5	0.63	1610	752	185	1120	128	14	10	8
47/86	37.1	0.57	2140	477	114	1550	191	10	6	8
48/86	37.8	0.21	628	588	3160	1030	107	8	3	4
49/86	37.2	0.61	1460	807	64	1070	191	12	5	9
50/86	36.2	0.40	909	1030	432	635	286	14	12	8
55/86	36.1	0.35	1540	692	46	640	156	14	71	590
56/86	36.2	0.37	1260	843	138	636	95	12	105	1280
57/86	34.2	0.45	906	3960	175	1270	684	20	333	1790
67/86	27.4	0.36	780	3340	107	42000	2100	12	18	47
68/86	31.3	0.32	618	5150	23	4040	800	17	10	52
69/86	28.0	0.66	7680	6480	46	9070	2610	19	26	102
70/86	30.8	0.60	2270	1650	28	30200	9560	22	12	37
71/86	27.2	0.74	1240	8920	151	6440	2390	31	34	76
72/86	35.9	0.44	2410	398	17	596	115	19	6	107
75/86	33.7	0.68	1910	2770	92	886	1090	16	23	70
76/86	36.2	0.59	2640	262	22	676	107	7	26	638
506	35.8	0.45	1860	631	41	635	163	14	13	158
507	35.2	0.43	727	2130	75	636	350	29	34	531
YY-511	35.8	0.49	1100	857	112	635	258	26	9	99

[a]n.d. = not determined

In addition ten random samples were checked for Co, Cr and Pb - but in all cases it was found to be below the limit of detection.

Table 2: Comparison of travertine uranium contents measured by DNA to the α-spectrometric method.

Sample	DNA (total uranium) uranium ppm	alpha-particle spectrometry (Acid leachable fraction) uranium ppm
506	2.2±0.1	2.05±0.07
7/86	4.5±0.2	3.17±0.07
40/86	2.5±0.1	2.43±0.06
52/86	1.5±0.1	1.20±0.10
53/86	0.9±0.1	0.72±0.02
60/86	2.7±0.1	2.29±0.06
74/86	0.9±0.1	0.84±0.04

Table 3: Ages and isotopic data

Sample	Th-230/Th-232	U-234/U-238	Th-230/U-234	Uranium ppm	Age x10^3 Corrected for an initial Th-230/Th-232 of: 0	1.5
16	>100	1.85±0.08	0.28±0.03	0.77±0.03	34±4	34
506	66±21	1.18±0.05	0.59±0.03	2.05±0.07	95±8	93
507	36±10	1.29±0.08	0.84±0.05	1.51±0.07	178±28	175
2/86	2±0.2	1.01±0.12	1.06±0.11	0.09±0.01	>300	>300
3/86	4±0.5	1.13±0.07	1.07±0.07	0.17±0.01	n.c.*	n.c.
4/86	8±1	1.18±0.12	0.93±0.08	0.11±0.01	$247\pm^{114}_{60}$	228
7/86	>100	1.14±0.03	0.94±0.03	3.17±0.07	$259\pm^{40}_{28}$	258
12/86 bot.	12±3	1.02±0.03	0.94±0.04	1.09±0.02	$260\pm^{47}_{32}$	244
12/86 top	15±4	1.08±0.05	0.93±0.04	0.82±0.03	$266\pm^{63}_{40}$	257
13/86	17±4	1.11±0.06	0.91±0.05	1.07±0.05	$237\pm^{58}_{38}$	228
14/86	92±35	0.99±0.08	0.94±0.08	1.60±0.11	$309\pm^{\infty}_{94}$	307
16/86	37±13	1.01±0.02	0.44±0.03	5.00±0.09	63±6	61
17/86	57±12	0.99±0.01	0.99±0.04	3.19±0.04	>300	>300
18/86	>100	1.03±0.03	1.00±0.04	3.76±0.10	>300	>300
19/86	>100	0.96±0.02	1.01±0.03	3.46±0.07	>300	>300
22/86	>100	1.00±0.04	1.00±0.05	2.09±0.08	>300	>300
23/86	>100	1.06±0.04	0.99±0.03	2.05±0.06	>300	>300
24/86	11±1	1.08±0.03	0.92±0.05	0.69±0.01	$254\pm^{64}_{42}$	240
25/86	13±2	1.15±0.07	1.31±0.10	0.73±0.03	n.c.	n.c.
26/86	28±3	1.10±0.03	0.92±0.02	1.18±0.03	$252\pm^{22}_{20}$	247
40/86	27±3	1.10±0.03	0.40±0.02	2.43±0.06	55±4	54
43/86	66±10	1.17±0.04	0.58±0.02	0.54±0.01	88±6	87
45/86	7±1	1.09±0.05	0.65±0.04	0.48±0.02	113±13	95
46/86	19±4	1.30±0.10	0.64±0.04	0.17±0.01	106±13	100
47/86	38±15	1.26±0.10	0.69±0.05	0.22±0.02	119±16	116
48/86	18±5	1.30±0.07	0.69±0.03	0.12±0.01	119±10	113
49/86	8±2	1.69±0.12	0.61±0.04	0.16±0.01	94±10	80
50/86	7±1	1.10±0.06	0.51±0.03	0.63±0.04	76±8	65
52/86	13±3	1.12±0.08	0.68±0.06	1.20±0.10	121±28	112
53/86	12±2	1.07±0.03	0.31±0.02	0.72±0.02	40±3	36
56/86	75±7	1.03±0.01	2.06±0.04	0.91±0.01	n.c.	n.c.
57/86	77±7	0.97±0.01	1.06±0.03	6.80±0.13	n.c.	n.c.
58/86	>100	1.05±0.02	0.95±0.04	2.45±0.05	$294\pm^{81}_{31}$	293
60/86	19±3	1.07±0.03	0.90±0.05	2.39±0.06	$231\pm^{42}_{31}$	224
67/86	20±3	0.94±0.03	1.21±0.10	9.15±0.43	n.c.	n.c.
70/86	18±3	0.94±0.02	0.97±0.05	1.92±0.04	n.c.	n.c.
72/86	78±18	1.17±0.05	0.87±0.04	0.62±0.02	198±25	196
74/86	11±3	1.13±0.08	0.67±0.06	0.84±0.04	117±19	107
75/86	11±1	1.03±0.04	0.71±0.03	2.27±0.09	132±13	121
76/86	>100	1.27±0.04	0.85±0.04	0.97±0.03	183±23	182

*n.c. = non calculatable

Appendix: Stratigraphic and topographic information

Sample No.	Locality	Figure ref.	Israel-grid coordinates	Lower[1] contact	Thickness where sampled (cm)	Elevation[2] above M.S.L. (m)	Elevation above active[2] erosional surface (m)	Comments[3]
16	Beer Menuha	Fig.7.A	1628/9687	E	-50	180	0-1	
2/86	En Erga	Fig.5.E	1676/0047	"	-200	-5	10	strongly tilted, sheared
3/86	En Erga	Fig.5.E	1677/0048	"	-150	15	25	dipping ESE: bottom

Appendix: Stratigraphic and topographic information

Sample No.	Locality	Figure ref.	Israel-grid coordinates	Lower[1] contact	Thickness where sampled (cm)	Elevation[2] above M.S.L. (m)	Elevation above active[2] erosional surface (m)	Comments[3]
16	Beer Menuha	Fig.7,A	1628/9687	E	~50	180	0-1	
2/86	En Erga	Fig.5,E	1676/0047	"	~200	-5	10	strongly tilted, sheared
3/86	En Erga	Fig.5,F	1677/0048	"	~150	15	25	dipping ESE; bottom
4/86	En Erga	"	"	"	"	"	"	dipping ESE; top
7/86	En Zach	Fig.4,A	1696/0255	S	~40	-70	2	top
8/86	En Zach	"	"	"	"	"	"	bottom
12/86	Tributary of Nahal Hazeva	Fig.4,B	1666/0264	N	~140	65-70	25	max. thickness up to ~3m. bottom
13/86	"	"	"	"	"	"	"	middle
14/86	"	"	"	"	"	65-70	"	top
YY-511		"	"	"	?	"	"	precise location in section unknown
16/86	Tributary of Nahal Mashaq	Fig.4,C	1654/0225	"	~170	5	10-15	max. thickness up to ~4m. bottom
17/86	"	"	"	"	"	"	"	middle
18/86	"	"	"	"	"	"	"	top
YY-354	"	"	"	"	?	"	"	precise location in section unknown.
19/86	Upp. Nahal Mashaq	Fig.4,D	1647/0221	"	~550	40-45	40	bottom, lacustrine 1st. about 10m. above "upper erosional surface" of Sneh, 1982
20/86	"	"	"	"	"	"	"	
21/86	"	"	"	"	"	40-45	40	
22/86	"	"	"	"	"	"	"	
23/86	"	"	"	"	"	"	"	top
24/86	Upp. tributary of Nahal Mashaq	Fig.4,E	1651/0224	"	~220	30	20	bottom
25/86	"	"	"	"	"	"	"	middle
26/86	"	"	"	"	"	"	"	top
40/86	Makhtesh-Qatan	Fig.3,A	1701/0404	LC	~100	~15	6-8	upper erosional surface
43/86	"	"	"	"	"	"	"	"
45/86	"	Fig.3,B	1699/0405	"	~180	~10	"	upper erosional surface. max. thickness ~3m
46/86	"	"	"	"	"	"	"	"
47/86	"	"	"	"	"	"	"	"
48/86	"	"	"	"	"	"	"	"
49/86	"	Fig.3,C	1694/0412	"	~90	10	5	Lower erosional surface
50/86	"	"	"	"	"	"	"	"
52/86		Fig.3,D	1699/0410	"	~200	"	8	Upper erosional surface
53/86	"	"	"	"	"	"	"	"
55/86	Upp.Nahal Omer	Fig.6,A	1638/9937	S	~300	105	15-20	Upper erosional surface
56/86	"	"	"	"	"	"	"	"
57/86	"	"	"	"	"	"	"	"
58/86	"	Fig.6,B	1640/9937	"	~200	108	"	Upper erosional surface
60/86	"	"	"	"	"	"	"	"
67/86	Moah	Fig.6,C	1654/9944	"	~400	50	10-15	C; Upper erosional surface
68/86	"	"	"	"	"	"	"	"
69/86	"	"	"	"	"	"	"	M; "
70/86	"	"	"	"	"	"	"	O; "
71/86	"	"	"	"	"	"	"	C; "
72/86	"	"	"	"	"	"	"	"
74/86	Low. Nahal Omer	Fig.6,D	1653/9949	"	~100	40	4-6	Lower erosional surface
75/86	Nahal Shivyah	Fig.6,E	1658/9970	Q	~40	20	0.5	Buried by alluvial fan
76/86	"	Fig.6,F	1661/9968	"	~80	"	3-4	
506	Nahal Hiyyon	Fig.7,B	1626/9599	N-Q	~70	207	10	
507	"	"	"	"	~70	205	"	

1) J - Jurassic limestone; LC - Lower Cretaceous sandstone; S = Senonian chalk and marl; E = Eocene chalky - limestone; N = Neogene sandstones, silts and carbonates; Q = Quaternary clastic fill.

2) All elevations approximate.

3) Travertines, unless otherwise specified; L = lacustrine limestone; C = chalk; M = marl; O = plentiful organic material; Erosional levels refer to local drainage basin only and are not correlatable on a regional basis.

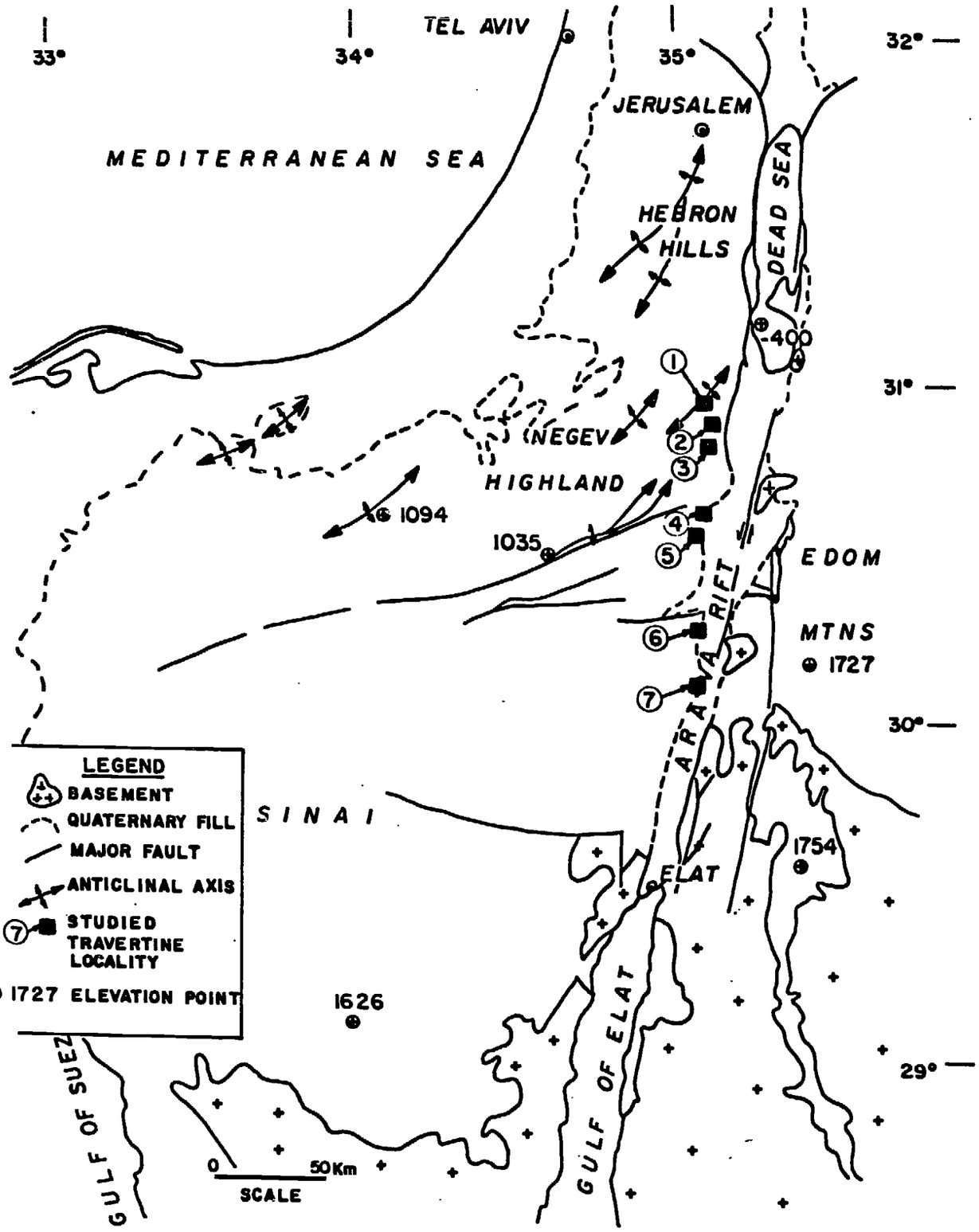
33°
34°
TEL AVIV
35°
32°
JERUSALEM
MEDITERRANEAN SEA
HEBRON HILLS
DEAD SEA
400
1
31°
2
3
NEGEV HIGHLAND
1094
1035
4
5
EDOM MTNS
1727
ARAVA RIFT
6
7
30°
LEGEND
BASEMENT
QUATERNARY FILL
MAJOR FAULT
ANTICLINAL AXIS
STUDIED TRAVERTINE LOCALITY
1727 ELEVATION POINT
SINAI
1754
ELAT
1626
GULF OF SUEZ
GULF OF ELAT
29°
0
50Km
SCALE

Fig. 1

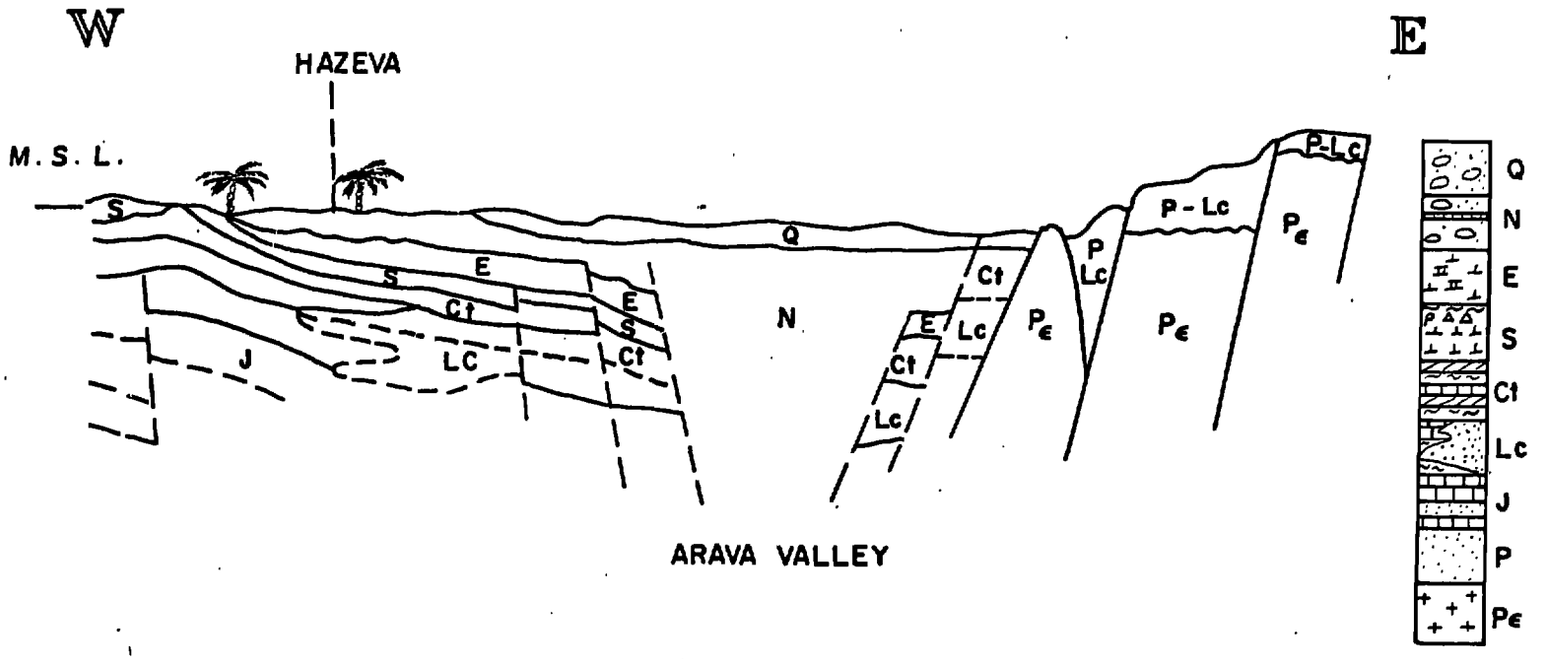
W
E
HAZEVA
M.S.L.
S
E
Ct
J
LC
Q
N
Ct
E
Lc
Pε
P
Lc
P-Lc
Pε
ARAVA VALLEY
Q
N
E
S
Ct
Lc
J
P
Pε

Fig. 2

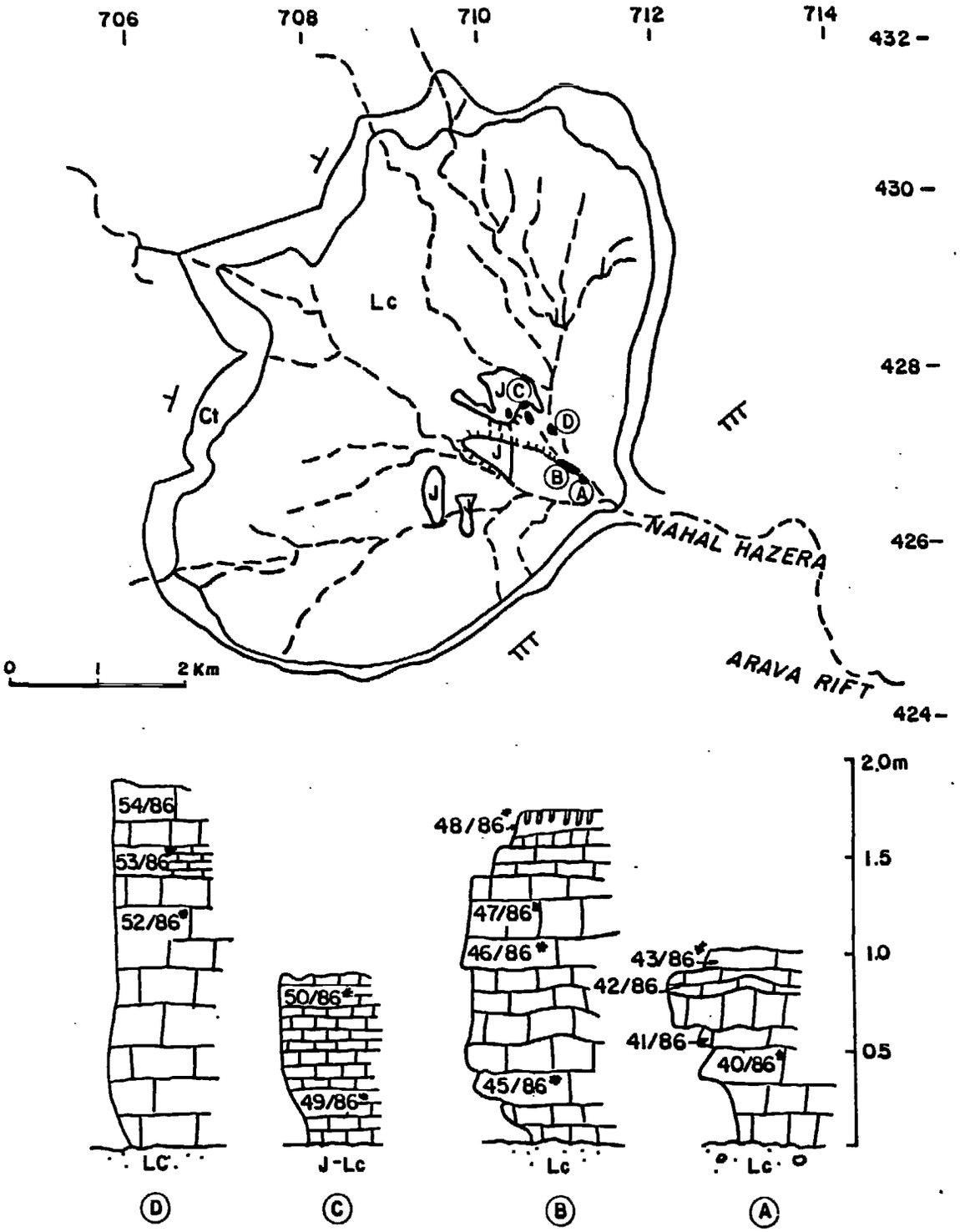
706
708
710
712
714
432
430
428
426
424
Lc
Ct
J
C
D
B
A
NAHAL HAZERA
ARAVA RIFT
0
1
2 Km
54/86
53/86
52/86
LC
50/86
49/86
J-Lc
48/86
47/86
46/86
45/86
Lc
43/86
42/86
41/86
40/86
Lc
2.0m
1.5
1.0
0.5
D
C
B
A

Fig. 3

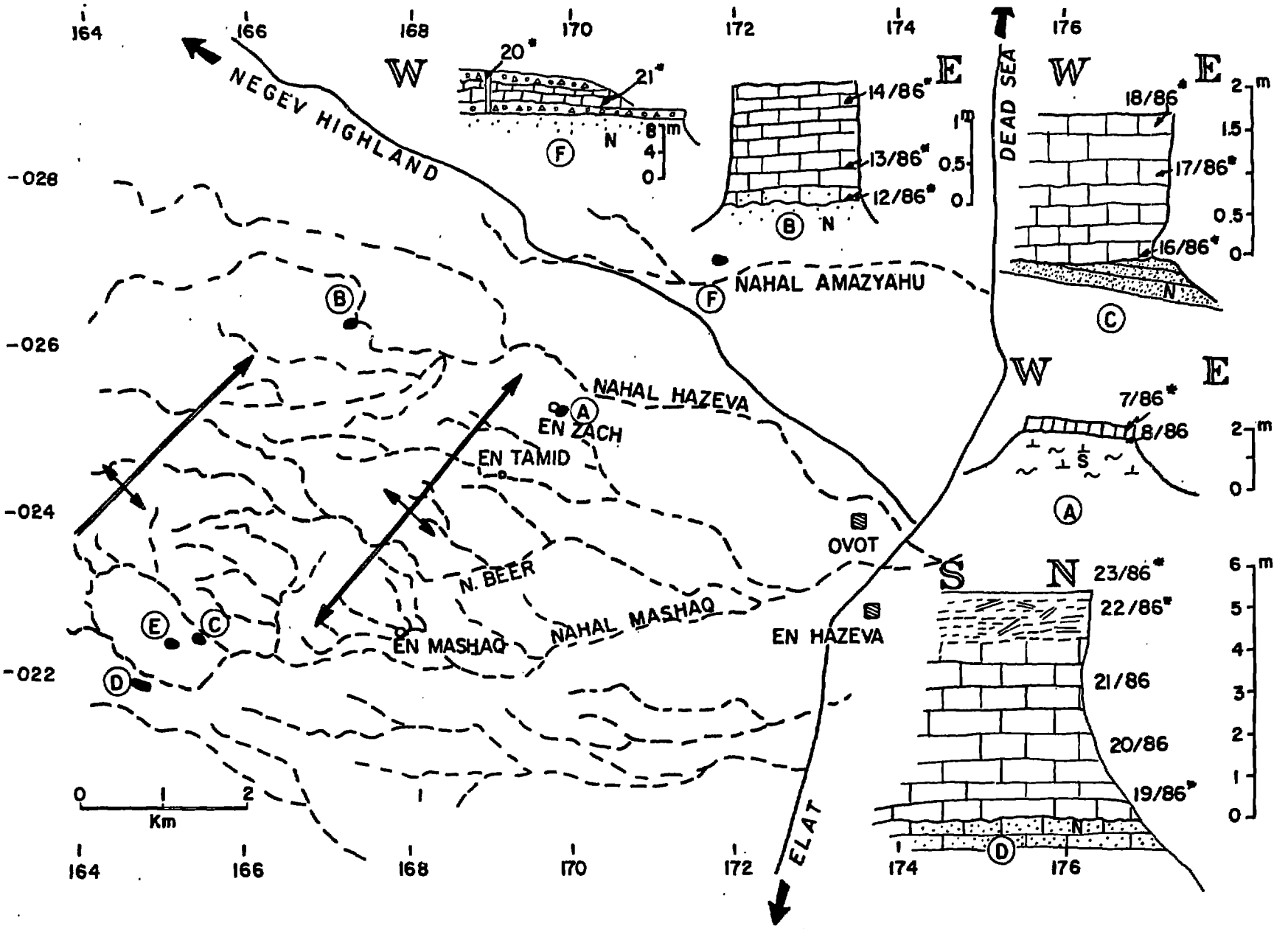
164
166
168
170
172
174
176
-028
-026
-024
-022
NEGEV HIGHLAND
DEAD SEA
NAHAL AMAZYAHU
NAHAL HAZEVA
EN ZACH
EN TAMID
N. BEER
NAHAL MASHAQ
EN MASHAQ
OVOT
EN HAZEVA
ELAT
Km
W
E
S
N
20*
21*
14/86*
13/86*
12/86*
18/86*
17/86*
16/86*
7/86*
8/86
23/86*
22/86*
21/86
20/86
19/86*
m

Fig. 4

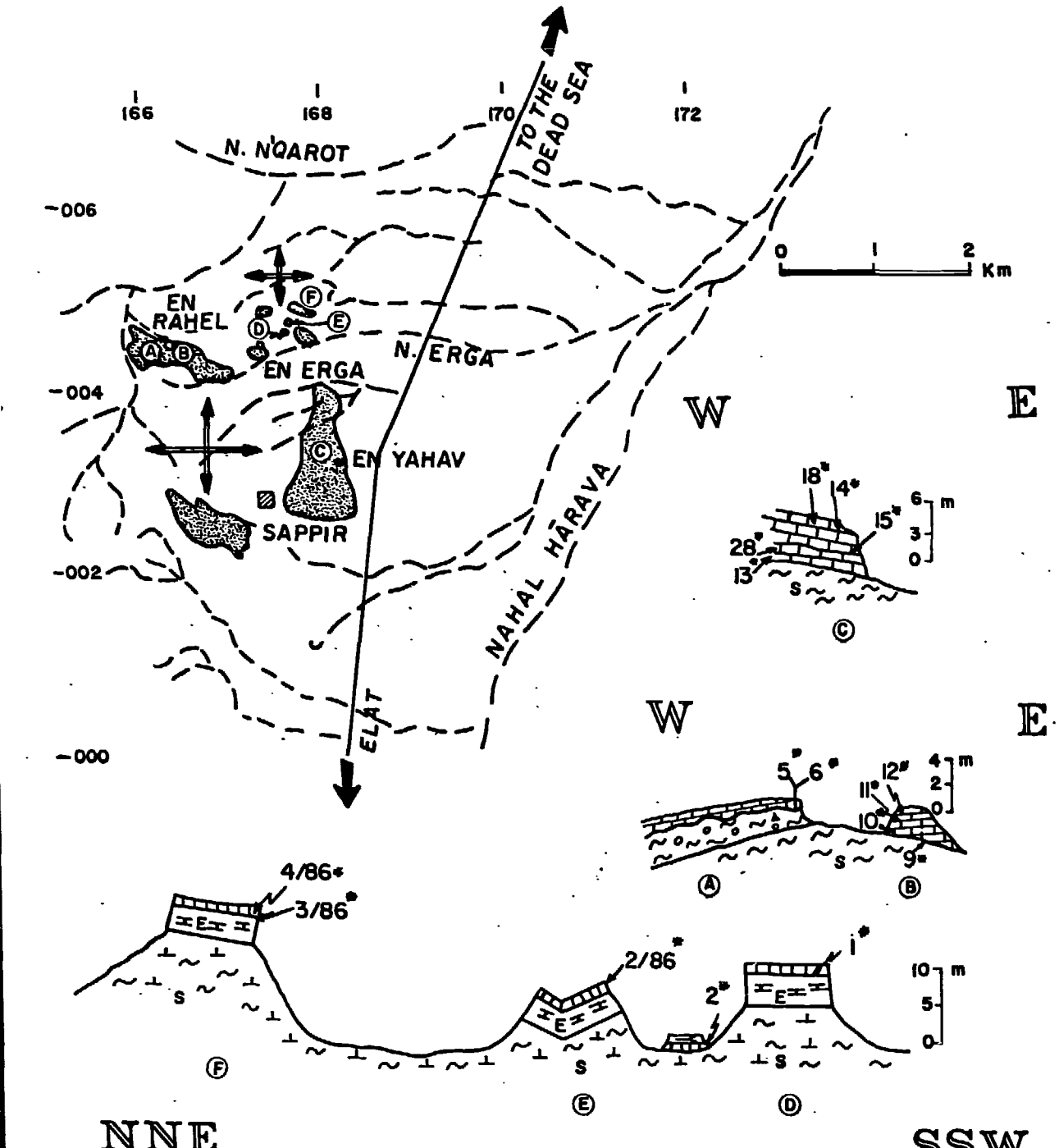
166
168
170
172
N. NQAROT
TO THE DEAD SEA
-006
-004
-002
-000
0 1 2 Km
EN RAHEL
EN ERGA
N. ERGA
EN YAHAV
SAPPIR
NAHAL HARAVA
ELAT
W E
18*
4*
15*
28*
13*
6
3
0
m
S
C
W E
5*
6*
12*
11*
10*
9*
4
2
0
m
A
B
4/86*
3/86*
2/86*
2*
1*
10
5
0
m
S
F
E
D
NNE
SSW

Fig. 5

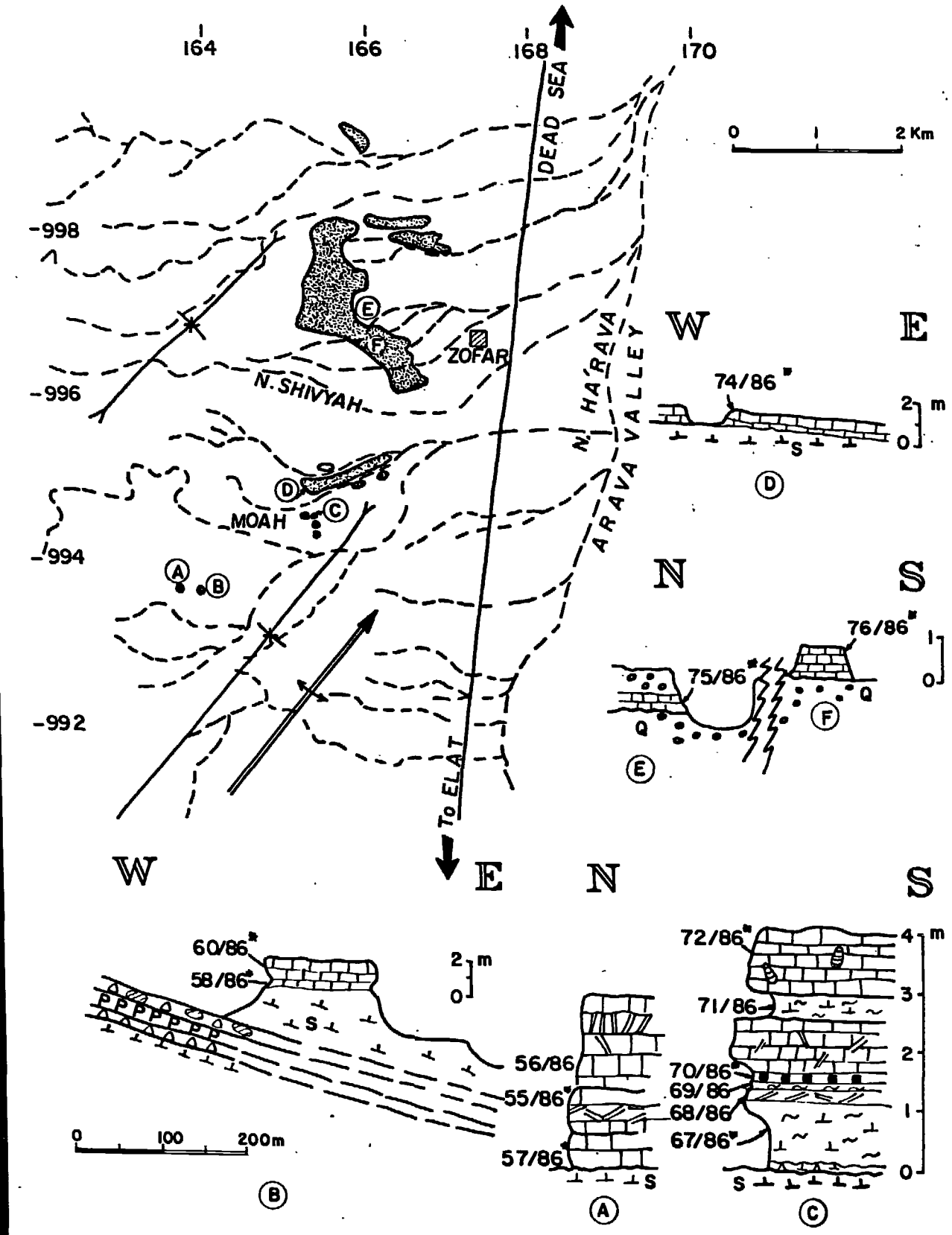
164
166
168
170
DEAD SEA
0 1 2 Km
-998
-996
-994
-992
E
F
ZOFAR
N. SHIVYAH
D
MOAH
C
A
B
To ELAT
N. HA'ARAVA
ARAVA VALLEY
W E
74/86
2 m 0
S
D
N S
76/86
75/86
1 m 0
Q
F
E
W E N S
60/86
58/86
2 m 0
S
56/86
55/86
57/86
0 100 200m
B
A
72/86
71/86
70/86
69/86
68/86
67/86
4 m 3 2 1 0
S
C

Fig. 6

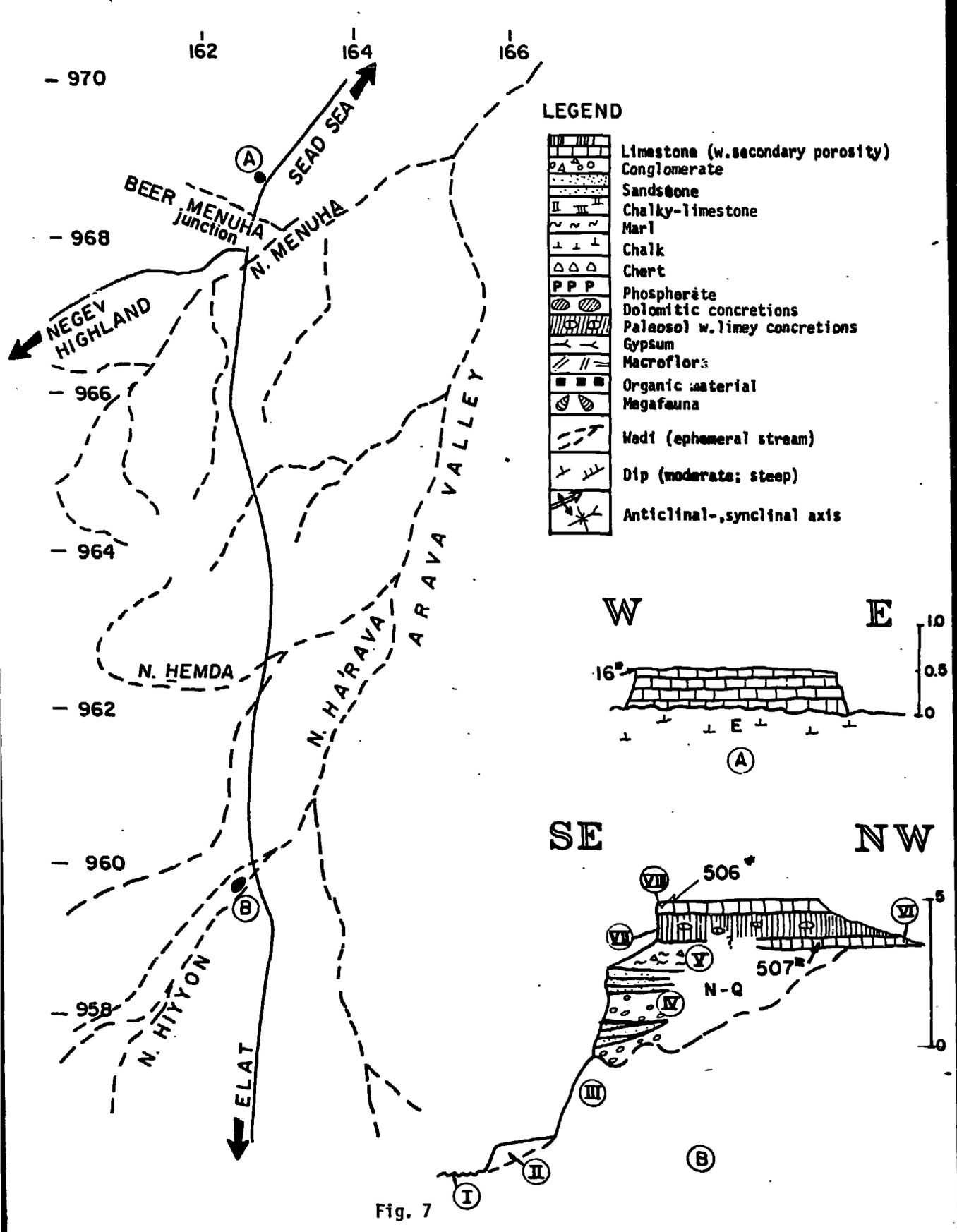
162
164
166
970
968
966
964
962
960
958
SEAD SEA
A
BEER MENUHA junction
N. MENUHA
NEGEV HIGHLAND
N. HEMDA
N. HA'RAVA
ARAVA VALLEY
N. HIYYON
ELAT
B
LEGEND
Limestone (w.secondary porosity)
Conglomerate
Sandstone
Chalky-limestone
Marl
Chalk
Chert
Phosphorite
Dolomitic concretions
Paleosol w.limey concretions
Gypsum
Macroflora
Organic material
Megafauna
Wadi (ephemeral stream)
Dip (moderate; steep)
Anticlinal-,synclinal axis
W
E
16°
E
1.0
0.5
0
A
SE
NW
506°
507°
VII
VI
V
IV
III
II
I
N-Q
5
0
B

Fig. 7

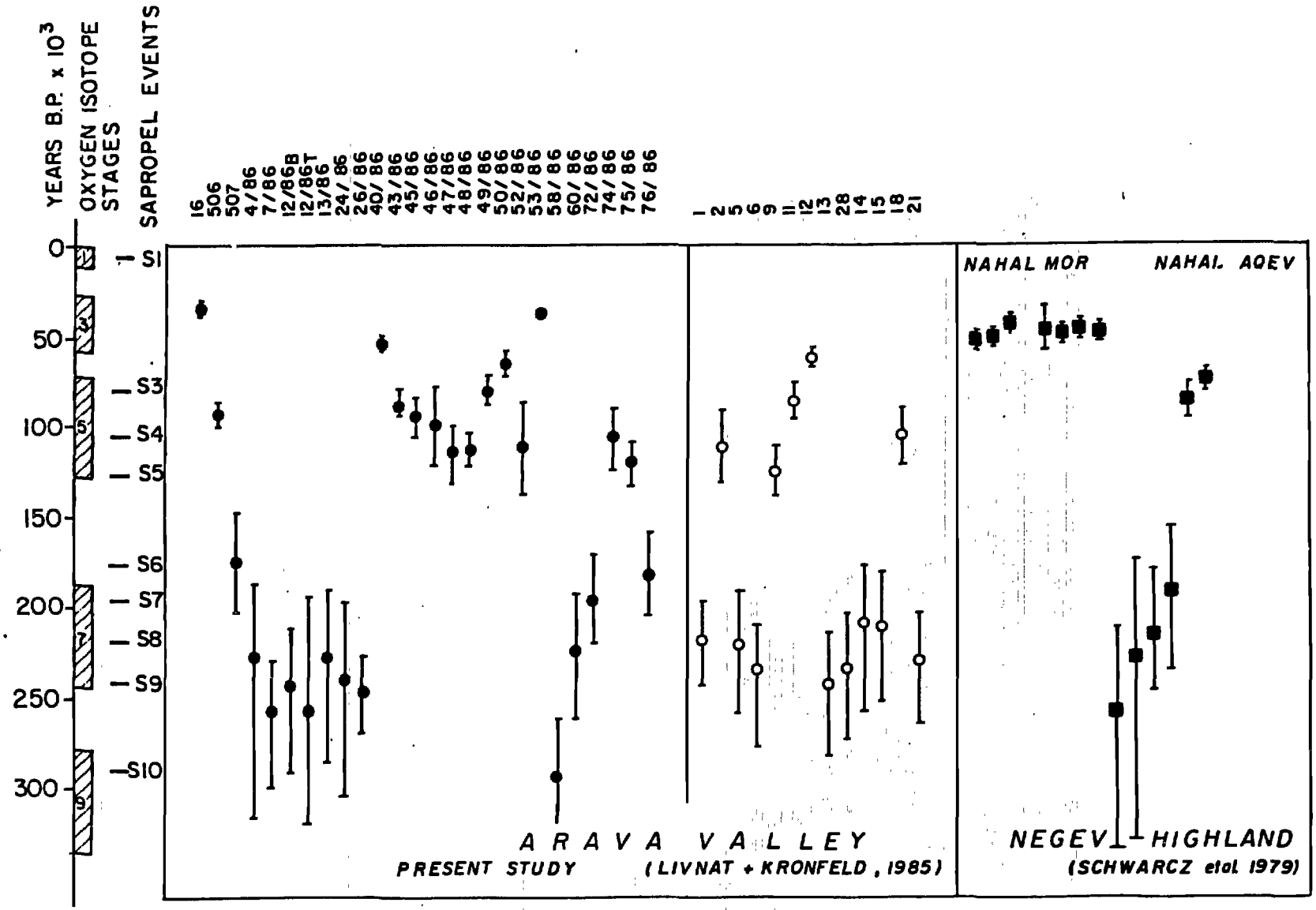
YEARS B.P. x 10³
OXYGEN ISOTOPE STAGES
SAPROPEL EVENTS
0
50
100
150
200
250
300
1
3
5
7
9
S1
S3
S4
S5
S6
S7
S8
S9
S10
16
506
507
4/86
7/86
12/86B
12/86T
13/86
24/86
26/86
40/86
43/86
45/86
46/86
47/86
48/86
49/86
50/86
52/86
53/86
58/86
60/86
72/86
74/86
75/86
76/86
1
2
5
6
9
11
12
13
28
14
15
18
21
NAHAL MOR
NAHAL AQEV
ARAVA VALLEY
PRESENT STUDY
(LIVNAT + KRONFELD, 1985)
NEGEV HIGHLAND
(SCHWARCZ etal 1979)

Fig. 8